Two Different Approaches to a Macroscopic Model of a Bio-Inspired Robotic Swarm

Thomas Schmickl [a] Heiko Hamann [a,b] Heinz Wörn [b]
Karl Crailsheim [a]

[a] *Department for Zoology, Karl-Franzens-University Graz, Austria*

[b] *Institute for Process Control and Robotics, Universität Karlsruhe (TH), Germany*

Abstract

By compiling macroscopic models we analyze the adaptive behavior in a swarm of autonomous robots generated by a bio-inspired, distributed control algorithm. We developed two macroscopic models by taking two different perspectives: A Stock & Flow model, which is simple to implement and fast to simulate, and a spatially resolved model based on diffusion processes. These two models were compared concerning their prediction quality and their analytical power: One model allowed easy identification of the major feedback loops governing the swarm behavior. The other model allowed analysis of the expected shapes and positions of observable robot clusters. We found a high correlation in the challenges posed by both modeling techniques and we highlighted the inherent problems of inferring emergent macroscopic rules from a microscopic description of swarm behavior.

Key words: macroscopic modeling, swarm robotics, bio-inspired robotics

1 Introduction

Swarm robotics [5, 27], which is the robotic application of swarm intelligence [1, 13, 3], is an emerging field of science characterized by a high degree of interdisciplinarity. An ever-increasing variety of projects tries to solve the major key problems of autonomously interacting moving machines (robots), which are: complexity, noise tolerance, adaptability and predictability of collective behavior. Most of these projects are performed by interdisciplinary teams to tackle these problems from several scientific directions simultaneously and cooperatively [18, 26]. These teams often include engineering scientists, mathematicians, physicists and biologists. The approaches pursued to develop the

robot controllers are also manifold. Evolutionary Algorithms [30], potential field methods [15], and hand-coded bio-inspired algorithms [20] are applied. The idea of investigating bio-inspired control algorithms is based on the fact that interacting groups of organisms (swarms, herds, flocks) are frequently found in nature [21]. These forms of collective behavior emerged by natural selection [6] during millions of years of biological evolution and can, therefore, be assumed to be well shaped and well adapted to the ecological constraints of the animals that show these behaviors. By translating these behavioral principles to robotic control programs, stable and efficient robotic swarms can be formed. Whereas these control programs act in environments that are comparable to the environment of the focal real-world organisms. Additionally, the robotic swarm can also serve as a sort of a hardware simulation of the biological source of inspiration. In this way, it can be used as a valuable tool to investigate and to understand biological swarm systems. For both of these approaches, the identification and the understanding of key factors shaping the swarm behavior and other global swarm properties are crucial for achieving valuable scientific results. As these systems are multi-component systems consisting of many cooperating agents, the basic key factors reside within the agent-to-agent interactions. It is the composition of distributed feedback loops (negative and positive) being responsible for the resulting collective swarm behaviors.

Often bottom-up simulation (individual-based or embodied simulation) is used to simulate swarm behavior on a computer. These microscopic models have frequently turned out to be an imperfect tool for identifying and analyzing these feedbacks: Such simulations are often too much focused on mimicking the overall collective behaviors instead of incorporating all relevant proximate mechanisms. Unfortunately, the predicted collective swarm behavior might result from simulation artifacts, hidden behind the high complexity of these individual based simulations. Additionally, bottom-up simulations suffer from computational complexity, not allowing decent and exhaustive parameter sweeps within reasonable time.

In contrast, macroscopic models involving a higher level of abstraction, are easier to understand, easier to analyze (parameter sweeps, sensitivity analysis) and can possibly reveal a few intrinsic parameters of the system strongly affecting or even governing the swarm behavior.

In general, the purpose of macroscopic models in swarm robotics is to support the algorithm design phase as the design of individual-/micro-level algorithms, that result in the desired swarm-/macro-behavior, has proven to be challenging [11, 17]. One option to overcome this problem is the modeling approach. In swarm robotics there is only a small variety in mature state-of-the-art models that are ready to support the algorithm design phase. The presumably mostly used approach is based on rate equations (e.g., see [17, 4]). A drawback of

these rate equation approaches is the limited representation of space – either homogeneous space is assumed or a rough discretization by states is done (nevertheless, in [9] a conceptual approach is reported showing a generalization of the rate equation approach to continuous space). In addition to the rate equation approaches, several other preliminary and rather specialized models were proposed: In [31] a formal method using temporal logic to specify emergent swarm behavior is presented. In [28] a model for a special aggregation behavior is analytically derived by applying combinatorics and linear algebra. In [2] a model for a special case of a collective motion algorithm [19] is presented. For a more detailed review of swarm models with focus on swarm robotics see [11].

Both models, that are presented in this paper, are macroscopic and have potential to be generalizable. The idea of this modeling approach is to predict the macroscopic behavior based on the control algorithm, which is a microscopic description. The most relevant quantity, that is predicted by the models, is number of robots (or robot density) at areas of interest.

2 The Robotic Swarm – Empiric Experiments

The focal scenario of our modeling approach was a series of empiric experiments performed with a swarm of 15 mobile and autonomous Jasmine robots [16]. These robots were controlled by a bio-inspired algorithm, that is called 'BEECLUST' and that was derived from honeybees' navigation behavior in a temperature gradient. For details of this study, please see [22, 23, 14]. For transferring the honeybees' behavior to a robotic swarm, the temperature gradient was translated into a light gradient emitted by lamps mounted above the arena. In these experiments the collective decision making ability of the swarm was investigated by testing, whether or not the robots were able to preferentially aggregate below the brightest available light spot. In the following we define the investigated control algorithm BEECLUST (see also figure 1):

(1) All robots move (ideally) in straight lines.
(2) If a robot detects an object in front by analyzing reflections of emitted infrared (IR) pulses it stops and listens for IR signals without emitting pulses.
(3) If there are no relevant IR signals, the robot assumes the object to be an obstacle (e.g. the arena wall), turns randomly and continues with step 1.
(4) If the robot detects foreign IR signals, it assumes the object in front to be another robot. The stopped robot then measures the local luminance. The higher the luminance, the longer it waits at that place.
(5) After the waiting time has elapsed, the robot turns and continues with step 1.

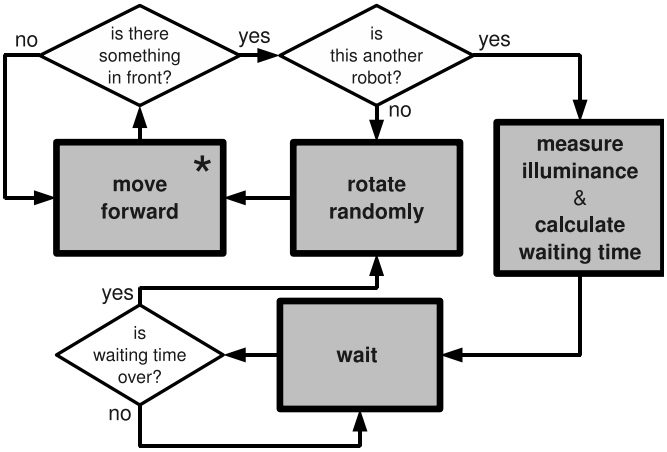

Fig. 1. Finite state machine describing the BEECLUST algorithm.

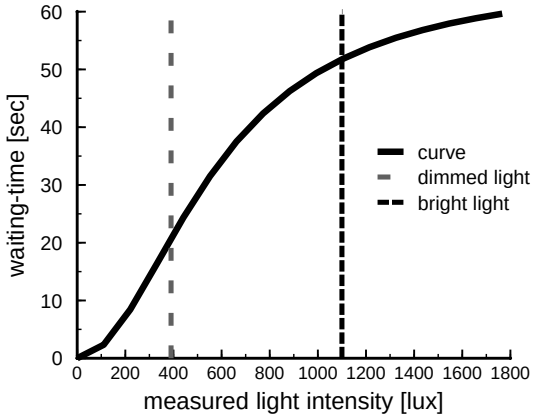

Fig. 2. The waiting time a robot waits after an encounter of another robot is non–linearly correlated with the measured local luminance. Robots measure this local luminance *only* after encounters with other robots. This curve is defined by equation 1, which is implemented in the robots' control algorithm (for more details see [23]).

The key components in this swarm robotic system are the number of robot-robot encounters and the dependency of the waiting time of a clustered robot on the locally measured luminance. A robot does only measure the light intensity, if it encounters another robot. Thus, a robot-robot encounter is the precondition to stop. The sigmoid correlation between the light intensity and the waiting time is depicted in figure 2.

Equation 1 shows, how the waiting time was implemented in the robotic control algorithm: w refers to the waiting time of a robot (in seconds), S refers to the luminance sensor values at the position of the robot. The sensor values scale linearly from 0 to 180 corresponding to 0 lux and approx. 1500 lux.

$$w = \frac{66S^2}{S^2 + 7000} \tag{1}$$

The study of [23] showed that this algorithm, which is very easy to implement on swarm robots, demonstrated impressive abilities of swarm intelligence in real hardware experiments. In an environment with one local and one global light maximum (emitted by two lamps) the robots preferentially aggregated at the spot with the higher luminance. At several points in time, the light intensities were changed (in four phases of 180 seconds each, see sun-like symbols in figure 5) and the robotic swarm quickly adapted its prior decision and reallocated robots between the two clusters to reach an adaptive and robust solution.

We adopted this experimental setup and constructed two abstract models of the swarm robotic systems. These models will allow to investigate (in future studies) several key components of that system without performing time-consuming experiments with real robot hardware. However, the plausibility of these macroscopic models has to be tested by comparing the model predictions to real empiric experiments, which is the main goal of the paper at hand. The models that we elaborate and analyze in this paper are easily extensible and adaptable. Thus the models will be useful not only for the special case of a specific swarm robotic experiment which we use as reference in our analysis here.

3 The Stock & Flow Model

To investigate the basic properties of the focal swarm robotic system, we constructed a very abstract macroscopic model of a swarm of 15 robots. The model depicts the control algorithm described above and was parameterized in a way to reflect the empiric experiments performed with the real robot hardware. We carefully incorporated all hardware parameters of the Jasmine robot (sensory radius, velocity, etc.) as well as all environmental parameters (arena dimensions, luminance on both sides of the arena, etc.). The model was constructed as a Stock & Flow model, depicting differential equations in a graphical way, following the concepts of system dynamics [8]. We used the modeling software Vensim$^{\text{TM}}$ [29] to construct and to evaluate the model. In Vensim$^{\text{TM}}$, *stocks* are the main components of a model, representing compartments that can hold quantities at a given time. In our model, these quantities are the number of robots which are always in one of the following three distinct states: aggregated on the left, or on the right side of the arena, or moving. The state transitions, that are shifts of quantities from one stock to another, are expressed by *flows* in such a model.

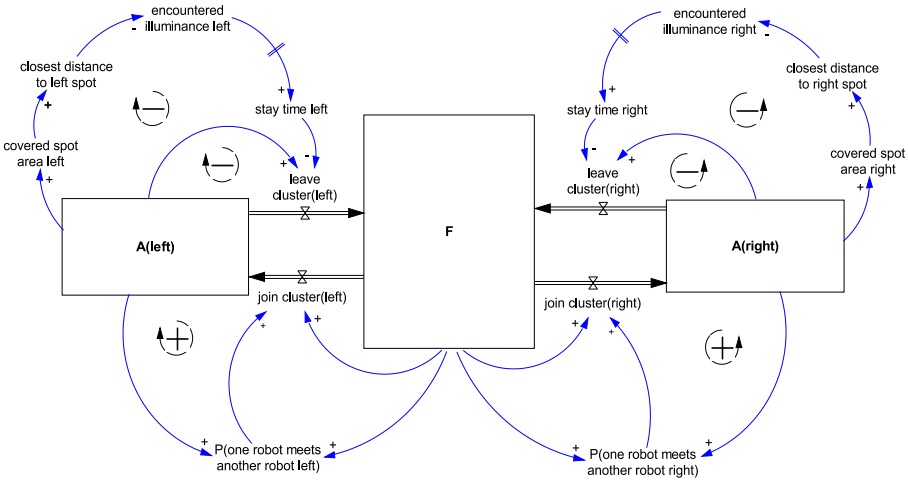

Fig. 3. Stock & Flow diagram of our model (simplified form). Stocks (compartments, boxes) describe the number of robots in one of the three main states (aggregated on the left/right side of the arena, or moving). Flows (rates, doubled arrows) model the changes from one compartment to the other (resulting from behavioral changes of individual robots). Thin arrows and variables without boxes describe auxiliary variables used to calculate the flows. Circular arrows highlight the major positive and negative feedback loops (indicated by the sign) that govern the behavior of the system. These feedback loops can be identified by following the thin arrows and flows in the Stock & Flow diagram.

Figure 3 depicts the basic components of our model. The change in the number of aggregated robots on the left side of the arena can be described by

$$\frac{dA_{\text{left}}}{dt} = J_{\text{left}}(t) - L_{\text{left}}(t). \tag{2}$$

The change in the number of robots on the right side of the arena is modeled in a similar way except for subscripts 'right' instead of 'left' (cf. Figure 3). The quantity (of robots) within this stock is changed by an inflow and an outflow [1] .

$J_{\text{left}}(t)$ is the number of robots joining the left cluster at time t, $L_{\text{left}}(t)$ is the number of robots leaving the left cluster at time t,

$$L_{\text{left}}(t) = \frac{A_{\text{left}}(t)}{w_{\text{left}}(t)}. \tag{3}$$

[1] Please note that our model contains also a variable $A_{\text{right}}(t)$, which represents the right stock in Figure 3. For the sake of simplicity, we describe only those equations that model the aggregation below the left lamp. The model is formulated symmetrically, so all variables having the index *left* have to replaced by the index *right* to model the other side of the arena.

The number of robots leaving a cluster depends primarily on the number of aggregated robots in the cluster ($A_{\text{left}}(t)$) and on the rate of change of this stock ($\frac{1}{w_{\text{left}}(t)}$). $w_{\text{left}}(t)$ is the current resting time of a robot in the left aggregation site, which depends on the local luminance measured by the robot when it joined the cluster. By taking up equation 1, we modeled the waiting time $w_{\text{left}}(t)$ for a robot joining the left cluster at time t as follows:

$$w_{\text{left}}(t) = 66\frac{S_{\text{left}}(t)^2}{S_{\text{left}}(t)^2 + 7000} \tag{4}$$

The reported sensor value $S_{\text{left}}(t)$ depends on the local luminance ($E_{\text{local,left}}(t)$) sensed by the robots at the point in time they joined the cluster. From our empiric experiments, we fitted the function $S_{left}(t)$ to model the sensor output in response to the encountered local luminance:

$$S_{\text{left}}(t) = \min\left(180, 256\frac{E_{\text{local,left}}(t)}{l_{\text{max}}}\right), \tag{5}$$

where $l_{\text{max}} = 1500\ lux$ represents the maximum luminance that can be encoded by the used luminance sensor.

To calculate the luminance below the lamp, several modeling steps had to be made. The luminance $E_{\text{max,left}}(t)$ at the spot directly below a lamp depends on the light intensity ($c_{\text{left}}(t) = 9$ *candela* for the dimmed light; $c_{\text{left}}(t) = 45$ *candela* for the bright light) emitted by the lamp's pulp, on the height of the lamp $h_{\text{left}} = 0.3m$ as well as on the shape of the lamps reflecting collector, which focuses the upwards reflected light beams in a sort of 'focus' ($f_{\text{left}} = 0.12m$) below the lamp.

$$E_{\text{left}}(t) = \frac{c_{\text{left}}(t)}{h_{\text{left}}^2} + \frac{c_{\text{left}}(t)}{(h_{\text{left}} - f_{\text{left}})^2} \tag{6}$$

Our model assumes that the clusters fill the spot below the lamps beginning at the center of the light spot (the brightest spot below the lamp). The more robots are already aggregated below a lamp, the lower is the luminance measured by additional robots that join the cluster, as they join the cluster in a bigger distance from the brighter central spot. Luminance decreases with quadratic decay with the distance from the light emitter. An implementation of this decay of luminance allowed us to model the saturation effect of light spots observable in empiric experiments.

As the clusters fill up with robots, the closest approachable distance $d_{\text{left}}(t)$ to the point below the lamp increases: The area covered with robots below

a lamp can be approximated by $\kappa_{\text{left}}(t) \approx A_{\text{left}} r_{\text{sensor}}^2 \pi$. The constant $r_{\text{sensor}} = 0.075m$ represents the range of the collision detection sensors. Assuming a radial arrangement of robots starting at the spot directly below the lamp, the minimum approach distance $d_{\text{left}}(t)$ for a robot is approximated by $d_{\text{left}}(t) \approx \sqrt{2\frac{\kappa_{\text{left}}(t)}{\pi}}$. Based on this, the maximum luminance at an already occupied site, which can be encountered by a joining robot, was modeled as

$$E_{\text{local,left}}(t) = \frac{c_{\text{left}}(t)}{h_{left}^2 + d_{\text{left}}(t)^2} + \frac{c_{\text{left}}(t)}{(h_{\text{left}} - f_{\text{left}})^2 + d_{\text{left}}(t)^2}. \tag{7}$$

One main problem in modeling the focal control algorithm on this highly abstract level was that the robots measure the luminance when they join the cluster and that they leave the cluster after a significant time delay that depends on the luminance they measured before. This means that the rate of leaving robots is a delayed effect of the luminance encountered in a variable period before. This problem is especially tricky in situations where the luminance changes spontaneously at a given time, as it was the case in the empiric experiments considered here. The best solution we found was to use a *smooth function* available in Vensim$^{\text{TM}}$, which calculates a gliding average throughout a time window of 66 seconds, which was the longest possible waiting time (see figure 2). This is expressed in our model by $\hat{w}_{\text{left}}(t) = smooth(w_{\text{left}}(x), (t-66) < x < t)$. This $\hat{w}_{\text{left}}(t)$ was used instead of $w_{\text{left}}(t)$ in equation 3 for those simulations that used the smooth function. We choose to use this smooth function instead of implementing this part of the system in higher detail because of the following reason: Modeling the 'memory' of each robot that is used for the time delay at the target would significantly increase the complexity of the model. As the Stock & Flow model's advantage is its simplicity, we think that the smooth-function is the best solution to find. Alternatively, one could implement a list that manages the waiting times of robots that arrive at the target spot in every time step. Such a model might be more precise and better grounded, but it will be a step from macroscopic modeling towards microscopic modeling, and would be unfavorable for our goals.

To complete equation 2, we also had to track the number of robots that join a cluster at time t in our model. We assumed, that free robots distribute equally in the arena, thus the fraction $\gamma = 0.5$ will be found on average on either one of the two sides of the arena.

$$J_{\text{left}}(t) = \gamma F_{\text{left}}(t) \varphi_{\text{left}}(t) P_{\text{detect}} \tag{8}$$

The number of robots that join a cluster depends on the number of free robots ($F(t)$), on the probability of robot-to-robot collisions ($\varphi_{\text{left}}(t)$) and on the

abilities of the robots to identify a robot-to-robot collision correctly ($P_{\text{detect}} = 0.5$).

The probability of robot-to-robot collisions is calculated by geometric considerations, mainly by calculating the proportions of the area covered by the sensors of a robot to the total available arena space:

The space covered by an aggregated robot is described by $\kappa_{\text{aggr}} = r^2_{\text{sensor}}\pi$. The space covered by a moving robot within a second is described by $\kappa_{\text{mov}} = r^2_{\text{sensor}}\pi + 2r_{\text{sensor}}v$. The constant $v = 0.3m/sec$ represents the robots' speed. $\kappa_{\text{arena}} = 1.5m^2$ represents the area of the arena.

Based on these calculations we modeled the likelihood of a focal robot to meet another robot (aggregated or free) on the corresponding side of the arena within one second (unit time step of the model).

$$\varphi_{\text{left}}(t) = \frac{\gamma F(t)\kappa_{\text{mov}} + A_{\text{left}}(t)\kappa_{\text{aggr}}}{0.5\kappa_{\text{arena}}} \tag{9}$$

Finally, the changes in the number of free robots ($F(t)$) are described by the rates of robots joining clusters and by the rates of robots leaving clusters

$$\frac{dF}{dt} = L_{\text{left}}(t) + L_{\text{right}}(t) - J_{\text{left}}(t) - J_{\text{right}}(t). \tag{10}$$

4 Spatial Model of Self-Propelled Particles

In this approach we followed the concept of Brownian agents as a model for swarm robots, that is, robots are seen as self-propelled particles showing random motion [24, 11, 12]. This approach is based on the idea that a microscopic description of the motion of a single robot can be set up: a stochastic differential equation – a Langevin equation. Based on the Langevin equation a macroscopic description of the particle density of the whole swarm is mathematically derived: a partial differential equation – the Fokker-Planck equation. For a very detailed description of this concept see [11].

Here, we omitted a strict derivation of a macroscopic model out of a microscopic model for simplicity and chose a phenomenological approach. Led by empirical arguments, we constructed two partial differential equations modeling the expected robot density for a given state depending on time and space. These equations are similar to those developed in the Stock & Flow model described in the previous section.

4.1 Spatially Modeling of Moving and of Waiting Robots

In our model, we distinguished two states: free (moving) robots F and aggregated robots A. Hence, we got two PDE; one for each state. Then we considered the density of free robots $F(\mathbf{x}, t)$ at position $\mathbf{x}$ in 2-d space and at time t. During an experiment, the density $F(\mathbf{x}, t)$ is, on the one hand, reduced by the number of robots which switch to the aggregated state. These transitions depend on a stopping rate $\varphi(\mathbf{x}, t)$ which is space- and time-dependent (as it depends on robot densities) and describes the ratio of stopping robots. On the other hand, $F(\mathbf{x}, t)$ is increased by beforehand stopped robots that switch to the moving state. These robots are that fraction of the stopped robots at $\mathbf{x}$ whose space-dependent waiting time $w(\mathbf{x})$ has elapsed at time t (provisionally we ignore dynamic waiting times). This fraction is equal to the fraction of robots which has stopped at time $t - w(\mathbf{x})$.

In addition to the above modeling of the state transitions, we needed to model the robots' motion. Following our previous works [11, 12] we chose a diffusion term as an abstract model of robot motion for several reasons:

(1) The robots' collision avoidance behavior shows features that are well modeled by diffusion processes: From time to time, the robots' movements are interrupted by encountering each other. This event can metaphorically be interpreted as colliding particles because both robots will change their direction after an encounter. However, an actual collision is avoided because the robots are programmed to turn away from each other before getting too close to each other. This turning angle can be considered being random due to the complex underlying processes in the sensors and due to the robots' imprecision. Furthermore, robots tend to move away from areas, which are crowded with free robots, into un-populated regions.
(2) Diffusion is mathematically easy to handle.
(3) Alternative macroscopic models of robot motion with similar or better performance seem not to be available.

Thus, we got the following partial differential equation that describes the change of the robot density of free robots over time

$$\begin{aligned}\frac{\partial F(\mathbf{x}, t)}{\partial t} =& D\nabla^2 F(\mathbf{x}, t) - F(\mathbf{x}, t)\varphi(\mathbf{x}, t)P_{\text{detect}} \\ &+ F(\mathbf{x}, t - w(\mathbf{x}))\varphi(\mathbf{x}, t - w(\mathbf{x}))P_{\text{detect}},\end{aligned} \tag{11}$$

for a diffusion constant $D = 500$ and probability $P_{\text{detect}} = 0.5$ of successfully detecting another robot. The first summand of the right hand side is the

diffusion term, which is our model of robot motion. The second and third summands describe state transition rates. The second summand describes the stopping robots (defined by the stopping rate $\varphi(\mathbf{x}, t)$) and, thus, reduces the density of free robots in $\mathbf{x}$ (negative influence). The third summand describes the robots that switch back to the moving state after their waiting time has elapsed (positive influence). The fraction of robots that start moving at time t is given by the fraction of stopping robots at time $t - w(\mathbf{x})$ (for the provisional simplification of a time-invariant waiting time $w(\mathbf{x})$).

We motivated the stopping rate $\varphi(\mathbf{x}, t)$ by empirical arguments. It is assumed to be proportional to the number of free robots populating the area covered by the sensors of free robots ($F(\mathbf{x}, t)\kappa_{\text{mov}}$) and on the number of aggregated robots populating the area covered by the sensors of an aggregated robot ($A(\mathbf{r}, t)\kappa_{\text{aggr}}$). These terms were approximated using densities which are normalized to a maximum density. We set the maximum density to $1/(\pi r_{\text{sensor}}^2)$ for the sensor range $r_{\text{sensor}} = 0.075m$. These normalized densities were obtained by $F_{\text{norm}}(\mathbf{x}, t) = F(\mathbf{x}, t)/(\pi r_{\text{sensor}}^2)$. As an approximation we got

$$\varphi(\mathbf{x}, t) = \left(F_{\text{norm}}(\mathbf{x}, t) \left(1 + \frac{2v}{\pi r_{\text{sensor}}} \right) + A_{\text{norm}}(\mathbf{x}, t) \right), \tag{12}$$

with nominal velocity $v = 0.3m/s$.

The equation for aggregated robots $A(\mathbf{x}, t)$ is directly obtained by omitting the diffusion term and inverting the sign of equation 11. It is in full correspondence to the Stock & Flow model:

$$\frac{\partial A(\mathbf{x}, t)}{\partial t} = F(\mathbf{x}, t)\varphi(\mathbf{x}, t)P_{\text{detect}} - F(\mathbf{x}, t - w(\mathbf{x}))\varphi(\mathbf{x}, t - w(\mathbf{x}))P_{\text{detect}}. \tag{13}$$

Note that equation 13 is mathematically not necessary (fully described by summations over time of F) but was introduced for demonstrative purposes.

In the scenario under investigation here, the waiting time $w(\mathbf{x}, t)$ was dynamic. Thus, the waiting times of robots having stopped at several different times in the past might elapse simultaneously. We had to sum robot fractions over all these times to model the state transition from aggregated to free correctly. The last summand of equation 11 (similarly for equation 13) became

$$\sum_{w' \text{ with } w(t')+t'=t} F(\mathbf{x}, t - w')\varphi(\mathbf{x}, t - w')P_{\text{detect}}. \tag{14}$$

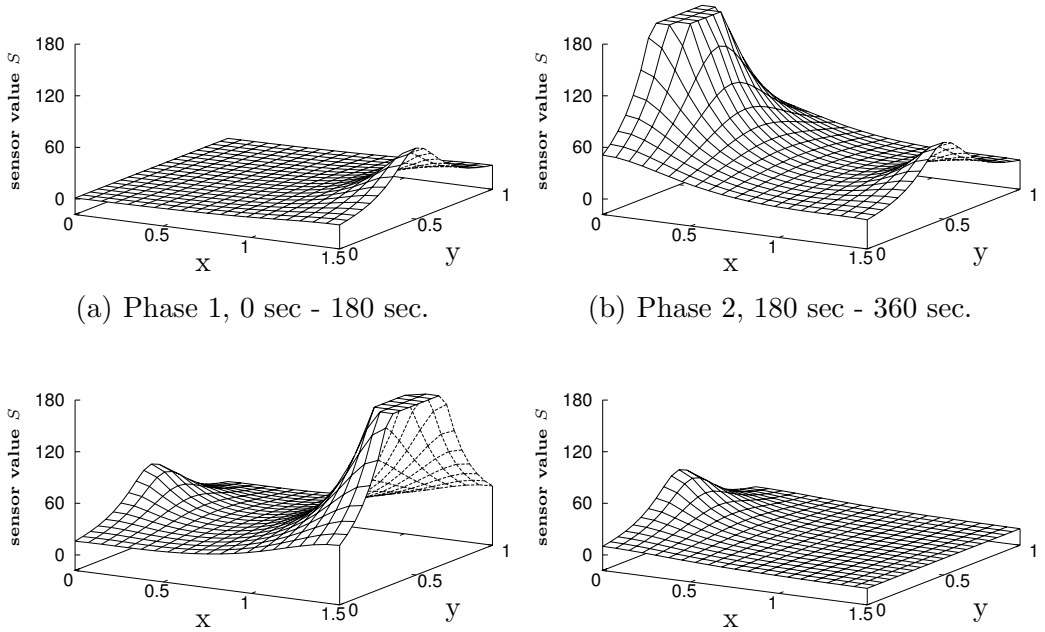

(a) Phase 1, 0 sec - 180 sec.

(b) Phase 2, 180 sec - 360 sec.

(c) Phase 3, 360 sec - 540 sec.

(d) Phase 4, 540 sec - 720 sec.

Fig. 4. Sensory map showing the sensor values as defined by equation 5 and 7 for the four phases of the experiment.

This is the sum of all robot fractions that stopped at any time $t' < t$ and for which is true: $w(t') + t' = t$ (i.e., the waiting time elapses at time t).

4.2 Initial Conditions and Boundary Conditions

Initially the robots were uniformly distributed (spatially homogeneous density). All of them were free robots; there were no stopped robots at the beginning. The borders were isolated, i.e. no robots leave and no robots enter the arena. We got an initial value problem which was solved numerically.

Most of the occurring parameters could be determined well, such as the spatial luminance distribution and the mapping of this luminance to sensor values. The diffusion constant D is a free parameter as it cannot be measured directly. In fact, it was used to adjust the homogenization speed of the moving robots density $F(\mathbf{x}, t)$. D adjusts the homogenization of the free robot density $F(\mathbf{x}, t)$ and indirectly only the quantity of aggregated robots; the qualitative features of the model are determined by the other parameters.

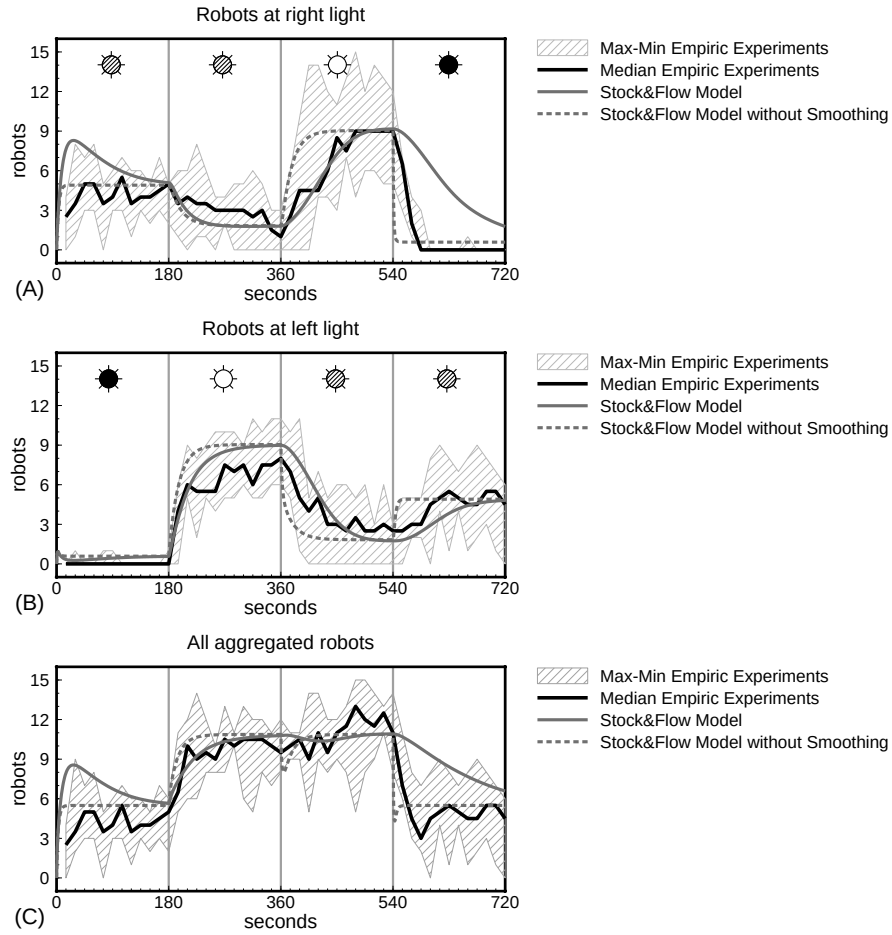

Fig. 5. Comparison for the empiric results achieved with real robotic hardware to the Stock & Flow model described in this article. The sun-like symbols indicate the light intensity emitted by the corresponding lamp: A black sun indicates that the lamp was turned off in this phase, a gray sun indicates that the lamp was set to low intensity and a white sun indicates that the lamp was set to high intensity. We compare the Stock & Flow model in two variants: with smoothing ($\hat{w}(t)$) and without smoothing ($w(t)$). N=6 repetitions per empiric experiment.

5 Results and Discussion

In figure 4 we present the sensory input spatially resolved as perceived by a robot according to our model (see equation 5 and 7). Note the plateaus at values of 180 which are caused by the min-function in equation 5.

In figure 5 the number of aggregated robots below the two lamps is given over time in all four consecutive phases of different environmental conditions (lamp configurations). The prediction of the Stock & Flow model closely follows the median aggregation levels observed with real robotic hardware, especially in the second and in the third experimental phase. Two major deviations of

the model are prominent and have to be investigated: At the initial phase, when only one dimmed light was present, the Stock & Flow model predicted an overshoot for the first two minutes. After that, the predicted number of aggregated robots nicely converged to the empirically observed level. And in the last phase, after the right light was turned off completely, the cluster at this side of the arena was predicted to shrink much slower than it was observed in the experiments. We simulated the model again without smoothing the encountered local luminance, i.e. we used $w(t)$ instead of $\hat{w}(t)$. After this change, the predictions in the first and in the last phase were much closer to the empiric results, but were less optimal in the second and in the third phase. Thus, we conclude that the two observed artifacts (overshoot and slow decay) were resulting from the (necessary) usage of the smooth function, which was used to introduce the microscopic waiting time 'memory' of a robot into our top-down model.

Also the spatial model predicted the observed levels of aggregation with good agreement to the observed empiric results (see figure 6). D was used to fit the model for quantitative consistency to the experiments. However, the predictions for the decay of aggregated robots at the dimmed light in the contention phase of the experiment (right light in phases two and three) were inaccurate. From the investigation of this problem we came to an interesting insight that robots leaving the dimmed light region get very fast to the bright light region. Therefore, it is crucial for a high degree of adaptivity in the swarm behavior that the robots turn away from the cluster after the waiting time has elapsed. Furthermore, it is also important that the experiments were performed with a low robot density. However, by using a diffusion term for the robot motion the robot flow between the two lights is systematically too small in our model compared to the empiric data. Due to the low robot densities and the rather deterministic control algorithm, diffusion does not fully catch the actual quality of the observed behavior. This could only be resolved by dropping the diffusion approach and turning to (probably much) more complex approaches. But there seems to be a lack of applicable alternative macroscopic theories with an explicit spatial representation.

In both models the stopping rate $\varphi(t)$ (probability of robot-robot encounters) and the probability of successful robot-robot detection P_{detect} proved to be crucial indicating the importance of these key parameters. By discretizing the spatial model for using a numerical solver it can be considered an extremely finer grained variant of the Stock & Flow model which can, in return, be seen as a most coarsely variant of the spatial model.

One aspect of the swarm system that cannot be described with the Stock & Flow model is the position, the spatial expansion and the shape of the emerging clusters. At least partially, this information can be predicted by the spatial model. In figure 7 we compare the prediction of the spatial model for the robot

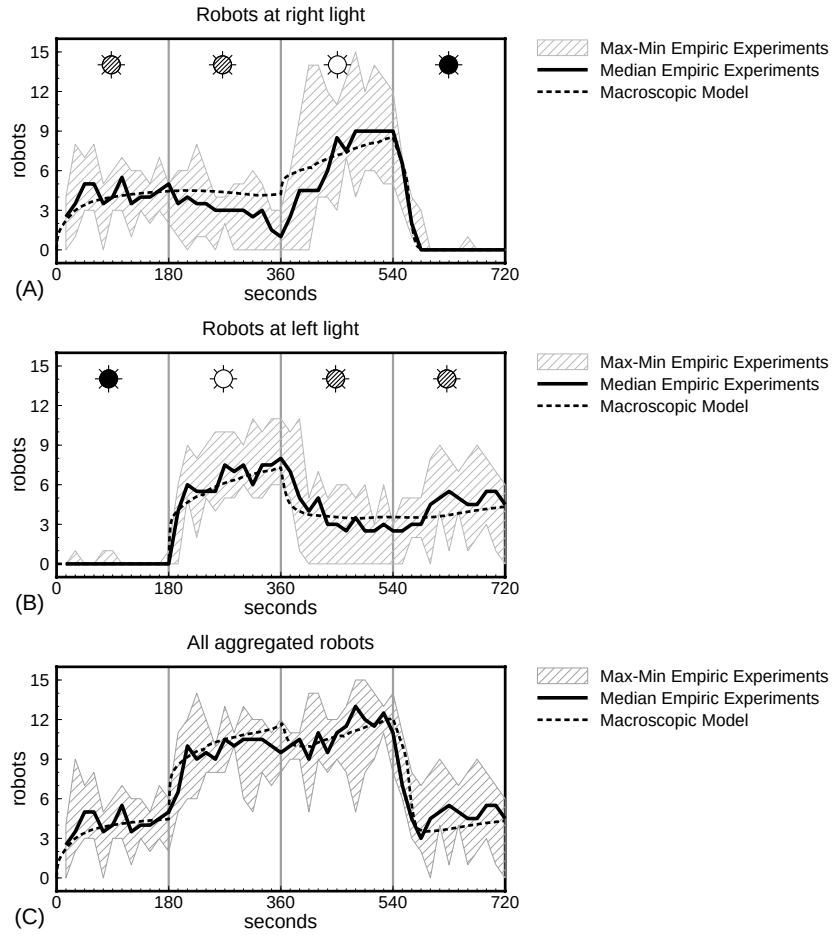

Fig. 6. Comparison for the empiric results achieved with real robotic hardware to the spatial model described in this article. The sun-like symbols indicate the light intensity emitted by the corresponding lamp: A black sun indicates that the lamp was turned off in this phase, a gray sun indicates that the lamp was set to low intensity and a white sun indicates that the lamp was set to high intensity. N=6 repetitions per empiric experiment.

density to a photo of the experiment in phase two. This can not serve as a validation but sampling statistically significant robot densities from experiments would generate an immense overhead that has not been invested yet.

6 Conclusion

Our analysis showed that the focal swarm robotic system can be well described by different macroscopic model approaches. Both offered high prediction quality without extensive fitting procedures. The Stock & Flow model was not systematically fitted to the empiric data, it was just parameterized with obvious and measurable parameters like robot speed, sensory radius and arena

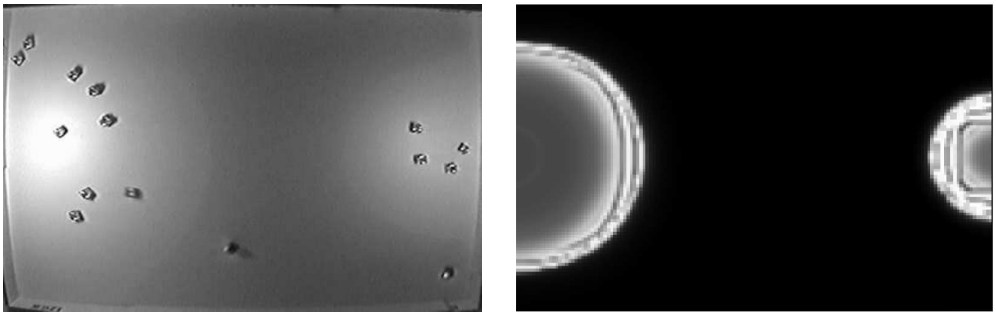

(a) Photo of the arena showing a typical configuration.

(b) Expected density of aggregated robots (higher densities are brighter).

Fig. 7. Comparing a swarm configuration observed during the experiments in phase two to the prediction of the spatial model. On the left side there is the brighter light compared to the dimmed light on the right.

dimensions. The advantage of the suggested macroscopic models is that they allow exhaustive parameter sweeps with low computational efforts. Both models evaluate a scenario within some seconds, thus many thousand simulation runs are not a problem of time.

Both models perform quite well in predicting the dynamics of robot aggregation at the target sites. The macroscopic model follows the empiric results more closely than the Stock & Flow model. When looking into details, a somehow different picture arises: In [23] we show a competition-effect that can be observed in the system: target spots compete for robots. This can be seen by the fact that the number of robots aggregated at dimmed spots depends on the luminance conditions on the other spot. In reaction to changes on the other target, the number of robots changed even at targets with unchanged quality. This effect was correctly predicted by the Stock & Flow model and was missing in the macroscopic model.

Both models can be easily adapted to other experiments performed with the BEECLUST algorithm. Changes in the size of the environment and in the number of used robotic modules can be made. Although the presented experiment is a classical 'choice' experiment, which is frequently used to investigate swarm-intelligent systems [25, 7, 3, 10], other environmental conditions are possible as well: For example, there could be more sub-optimal target spots present in the environment. Such changes are easier to implement using the spatially resolved macroscopic model. The main advantage of the Stock & Flow model is it's simplicity and an addition of target spots will quickly increase the complexity of the model. Thus, it would loose it's main advantage.

The focal swarm algorithm is rather simple, but, as was discussed in [23], the resulting collective behavior of the swarm is complex. Both macroscopic models discussed here allow to reduce this complexity by abstraction without losing the ability to make interesting predictions of characteristic key aspects

of the swarm behavior.

Acknowledgments

All authors are supported by the EU-IST-FET project 'SYMBRION', no. 216342 and the EU-ICT project 'REPLICATOR', no. 216240. Hamann is supported by the German Research Foundation (DFG) within the Research Training Group GRK 1194 Self-organizing Sensor-Actuator Networks. Schmickl is supported by the following grants: EU-IST FET project I-SWARM, no. 507006 and the FWF research grant Temperature-induced aggregation of young honeybees, no. P19478-B16.

References

[1] G. Beni. From swarm intelligence to swarm robotics. In E. Şahin and W. M. Spears, editors, *Swarm Robotics - SAB 2004 International Workshop*, LNCS, pages 1–9, Santa Monica, CA, July 2005.

[2] J. D. Bjerknes, A. Winfield, and C. Melhuish. An analysis of emergent taxis in a wireless connected swarm of mobile robots. In *IEEE Swarm Intelligence Symposium*, pages 45–52, Los Alamitos, CA, 2007. IEEE Press.

[3] E. Bonabeau, M. Dorigo, and G. Theraulaz. *Swarm Intelligence: From Natural to Artificial Systems*. Oxford Univ. Press, 1999.

[4] N. Correll and A. Martinoli. System identification of self-organizing robotic swarms. In M. Gini and R. Voyles, editors, *Proceedings of the 8th Int. Symp. on Distributed Autonomous Robotic Systems (DARS'06)*, pages 31–40, Berlin, Germany, 2006. Springer-Verlag.

[5] E. Şahin. Swarm robotics: From sources of inspiration to domains of application. In E. Şahin and W. M. Spears, editors, *Swarm Robotics - SAB 2004 International Workshop*, volume 3342 of *LNCS*, pages 10–20, Berlin, Germany, 2005. Springer-Verlag.

[6] C. Darwin. *On the Origin of Species By Means of Natural Selection*. John Murray, London, 1859.

[7] J.-L. Deneubourg, S. Aron, S. Goss, and J. M. Pasteels. The self-organizing exploratory pattern of the argentine ant. *Journal of Insect Behavior*, 3:159–168, 1990.

[8] J. W. Forrester. *World Dynamics*. Wright-Allen, Cambridge, Massachusetts, 1971.

[9] A. Galstyan, T. Hogg, and K. Lerman. Modeling and mathematical analysis of swarms of microscopic robots. In *Proceedings of IEEE Swarm Intelligence Symposium (SIS-2005), Pasadena, CA*, pages 201–208, Los Alamitos, CA, June 2005. IEEE Press.

[10] S. Garnier, C. Jost, R. Jeanson, J. Gautrais, M. Asadpour, G. Caprari, and G. Theraulaz. Aggregation behaviour as a source of collective decision in a group of cockroach-like-robots. In M. Capcarrere, editor, *Advances in artificial life: 8th European conference, ECAL 2005*, volume 3630 of *LNAI*, pages 169–178. Springer, September 2005.

[11] H. Hamann. *Space-Time Continuous Models of Swarm Robotics Systems: Supporting Global-to-Local Programming*. PhD thesis, University of Karlsruhe, Germany, November 2008.

[12] H. Hamann and H. Wörn. A space- and time-continuous model of self-organizing robot swarms for design support. In *First IEEE International Conference on Self-Adaptive and Self-Organizing Systems (SASO'07), Boston, USA, July 9-11*, pages 23–31, Los Alamitos, CA, July 2007. IEEE Press.

[13] J. Kennedy and R. C. Eberhart. *Swarm Intelligence*. Morgan Kaufmann, 2001.

[14] S. Kernbach, R. Thenius, O. Kornienko, and T. Schmickl. Re-embodiment of honeybee aggregation behavior in an artificial micro-robotic swarm. *Adaptive Behaviour*, 17:237–259, 2009.

[15] O. Khatib. Real-time obstacle avoidance for manipulators and mobile robots. *International Journal of Robotics Research*, 5:90–98, 1986.

[16] S. Kornienko, O. Kornienko, and P. Levi. IR-based communication and perception in microrobotic swarms. In *Proceedings of the IEEE/RSJ International conference on intelligent robots and systems (IROS'05), Edmonton, Canada*, Los Alamitos, CA, 2005. IEEE Press.

[17] A. Martinoli. *Swarm Intelligence in Autonomous Collective Robotics: From Tools to the Analysis and Synthesis of Distributed Control Strategies*. PhD thesis, Ecole Polytechnique Fédérale de Lausanne, 1999.

[18] F. Mondada, L. M. Gambardella, D. Floreano, S. Nolfi, J.-L. Deneubourg, and M. Dorigo. The cooperation of swarm-bots: Physical interactions in collective robotics. *IEEE Robotics & Automation Magazine*, 12(2):21–28, June 2005.

[19] J. Nembrini, A. F. T. Winfield, and C. Melhuish. Minimalist coherent swarming of wireless networked autonomous mobile robots. In B. Hallam, D. Floreano, J. Hallam, G. Hayes, and J.-A. Meyer, editors, *Proceedings of the seventh international conference on simulation of adaptive behavior on From animals to animats*, pages 373–382, Cambridge, MA, USA, 2002. MIT Press.

[20] D. Payton, M. Daily, R. Estowski, M. Howard, and C. Lee. Pheromone robotics. *Autonomous Robots*, 11(3):319–324, Nov. 2001.

[21] C. W. Reynolds. Flocks, herds, and schools. *Computer Graphics*, 21(4):25–34, 1987.

[22] T. Schmickl and H. Hamann. BEECLUST: A swarm algorithm derived from honeybees. In Y. Xiao and F. Hu, editors, *Bio-inspired Computing and Communication Networks*. Routledge, January 2010.

[23] T. Schmickl, R. Thenius, C. Möslinger, G. Radspieler, S. Kernbach, and

K. Crailsheim. Get in touch: Cooperative decision making based on robot-to-robot collisions. *Autonomous Agents and Multi-Agent Systems*, 18(1):133–155, February 2008.

[24] F. Schweitzer. *Brownian Agents and Active Particles. On the Emergence of Complex Behavior in the Natural and Social Sciences*. Springer-Verlag, Berlin, Germany, 2003.

[25] T. D. Seeley, S. Camazine, and J. Sneyd. Collective decision-making in honey bees: how colonies choose among nectar sources. *Behavioral Ecology and Sociobiology*, 28(4):277290, April 1991.

[26] J. Seyfried and et al. The I-SWARM project: Intelligent small world autonomous robots for micro-manipulation. In E. Şahin and W. M. Spears, editors, *Swarm Robotics - SAB 2004 International Workshop*, pages 70–83, Berlin, Germany, 2005. Springer-Verlag.

[27] A. J. C. Sharkey. Swarm robotics and minimalism. *Connection Science*, 19(3):245–260, Sept. 2007.

[28] O. Soysal and E. Şahin. A macroscopic model for self-organized aggregation in swarm robotic systems. In E. Şahin, W. M. Spears, and A. F. T. Winfield, editors, *Swarm Robotics - Second SAB 2006 International Workshop*, volume 4433 of *LNCS*, pages 27–42, Berlin, Germany, 2007. Springer-Verlag.

[29] V. Systems. Vensim^{TM}. `http://www.vensim.com`.

[30] V. Trianni. *Evolutionary Swarm Robotics - Evolving Self-Organising Behaviours in Groups of Autonomous Robots*, volume 108 of *Studies in Computational Intelligence*. Springer-Verlag, Berlin, Germany, 2008.

[31] A. F. T. Winfield, J. Sav, M.-C. Fernández-Gago, C. Dixon, and M. Fisher. On formal specification of emergent behaviours in swarm robotic systems. *International Journal of Advanced Robotic Systems*, 2(4):363–370, 2005.